Numerical Modeling of the Unsteady Vapor Outflow from a Flat Surface Using Direct Numerical Solution of the Boltzmann Equation

O.I. Rovenskaya, I.V. Voronich

Moscow Institute of Physics and Technology, Department of Aeromechanics and Flight Engineering
16 Gagarin st, Zhukovsky, 140180, Russia

Abstract. The unsteady vapor expansion into vacuum from a flat surface is studied using the direct numerical solution method for the Boltzmann equation. Robust numerical algorithm for such class of problems is suggested. The flow structure and distributions of flow parameters are investigated for all the regimes.

INTRODUCTION

The problem of unsteady vapor outflow into vacuum from a flat surface is a classical problem of the rarefied gas dynamics. For the collisionless gas expansion, the self-similar analytical solution is well known [1]. Regimes characterized by appreciable influence of collisions between particles have been investigated theoretically and numerically using the direct simulation Monte-Carlo (DSMC) methods [2–4]. It is of interest to solve this problem using the direct numerical solution method [5] in the context of its applications to complex flows.

The considered flow type includes equilibrium as well as non-equilibrium regions, therefore, the method used must be conservative and must ensure that the collision integral vanishes under the conditions of local thermodynamical equilibrium. In this paper, the method developed by F.G. Tcheremissine is used for calculation of the Boltzmann collision integral [5]. For approximation of the convective part of the Boltzmann equation explicit first- and second-order accurate flux conservative schemes with the symmetrical time integration method are used in the framework of finite volume approach [6]. Application of the method to such a problem requires adjustment of algorithm components, such as computational grids in velocity space, an approximation of the convective operator and a collisional relaxation algorithm. Therefore, the choice of robust algorithm is of critical importance. For verification, main peculiarities of numerical data obtained herein are compared with the results [4].

PROBLEM STATEMENT

The computational domain is a space between the evaporating surface and the external boundary placed at the distance $L \sim 10^3 \lambda_w$, where λ_w – the mean free path defined by the conditions on the evaporating surface. Gas is considered as monatomic and the hard spheres model is used for description of particles elastic interactions.

At the initial time moment $t = 0$, there are no particles in the computational domain and the distribution function equals zero. The distribution function for evaporating particles at $x = 0$ is taken to be constant and has the semi-maxwellian form

$$f(t,\mathbf{x},\boldsymbol{\xi})\big|_{x=0} = \frac{n_e}{(2\pi RT_w)^{3/2}} \exp\left(-\frac{\xi_x^2+\xi_y^2+\xi_z^2}{2RT_w}\right),\ \xi_x>0.$$

Here, n_e is the equilibrium vapor concentration, T_w is the surface temperature, ξ_x, ξ_y, ξ_z are particle velocity components, R is the gas constant. This condition implies that particles turning back to the surface do not affect

evaporating particles at the surface. At the external boundary $x = L$, the distribution function is set to be zero that is valid when flow does not reach this boundary. For further dimensional transformations, the characteristic time is defined as $\tau_0 = \lambda_w/v_0$, where λ_w is the mean free path for equilibrium evaporating gas and $v_0 = \sqrt{RT_w}$ is the characteristic velocity. Numerical calculations were carried out to the dimensionless time moment $t/\tau_0 = 300$ at which the continuum flow regime sets in.

NUMERICAL METHOD

The numerical method is based on direct numerical solution of the Boltzmann equation

$$\frac{\partial f}{\partial t} + \boldsymbol{\xi}\frac{\partial f}{\partial \mathbf{x}} = J(t,\mathbf{x},\boldsymbol{\xi}) = J(f,f) = \int_0^{2\pi}\int_0^{b_m}\int (f' f_*' - f f_*) g b db d\varepsilon d\boldsymbol{\xi}_* , \tag{1}$$

where $f = f(t,\mathbf{x},\boldsymbol{\xi})$ is the distribution function, $\boldsymbol{\xi}$, $\boldsymbol{\xi}_*$, $\boldsymbol{\xi}'$, $\boldsymbol{\xi}_*'$ are velocities of pair of particles before and after collision, $J(f,f)$ is the collision integral, $\mathbf{g} = \boldsymbol{\xi}_* - \boldsymbol{\xi}$ is the relative velocity, and b, ε are impact parameters. Introducing the velocity scale $v_0 = \sqrt{RT_w} = v_T/\sqrt{2}$, the length scale $\lambda_w = 1/(\sqrt{2}\pi n_e b_m^2)$ and the time scale $\tau_0 = \lambda_w / v_0 = \sqrt{2}\tau_T$ we obtain the dimensionless variables: $\tilde{\boldsymbol{\xi}} = \boldsymbol{\xi}/v_0$, $\tilde{t} = t/\tau_0$, $\tilde{b} = b/b_m$, $\tilde{\mathbf{x}} = \mathbf{x}/\lambda_w$, $\tilde{f} = f/(n_e v_0^{-3})$, where $v_T = \sqrt{2RT_w}$ is the thermal velocity. Equation (1) takes the form (further «˜» is omitted):

$$\frac{\partial \tilde{f}}{\partial \tilde{t}} + \tilde{\boldsymbol{\xi}}\frac{\partial \tilde{f}}{\partial \tilde{\mathbf{x}}} = \frac{1}{\sqrt{2}\pi} J(\tilde{f},\tilde{f}) . \tag{2}$$

For the discretization of (2), the 3D Cartesian grid $\{\boldsymbol{\xi}_\gamma\}$ with equidistant nodes is introduced in the velocity space, and the relevant grid $\{\mathbf{x}_i\}$ is introduced in the physical space. Consider the sphere of radius $V_{\max}$ that bounds the domain Ω in the velocity space. Suppose that the number of Cartesian nodes in the Ω domain is N_0.

Introducing of the grid values $f_\gamma(\mathbf{x}, t)$ and $J_\gamma(\mathbf{x}, t)$, the problem is to solve the set of equations for $f_\gamma(\mathbf{x}, t)$

$$\frac{\partial f_\gamma}{\partial t} + \boldsymbol{\xi}_\gamma \frac{\partial f_\gamma}{\partial \mathbf{x}} = \frac{1}{\sqrt{2}\pi} J_\gamma . \tag{3}$$

The calculation of the collision integral $J_\gamma(\mathbf{x}, t)$ at a point $\boldsymbol{\xi}_\gamma$ is based on the form [5, 7]

$$J_\gamma = J(t,\mathbf{x},\boldsymbol{\xi}_\gamma) = \frac{1}{4}\int\int_0^{2\pi}\int_0^{1}\int \phi(\boldsymbol{\xi}_\gamma)(f' f_*' - f f_*) g b db d\varepsilon d\boldsymbol{\xi}_* d\boldsymbol{\xi} , \tag{4}$$

where $\phi(\boldsymbol{\xi}_\gamma) = \delta(\boldsymbol{\xi} - \boldsymbol{\xi}_\gamma) + \delta(\boldsymbol{\xi}_* - \boldsymbol{\xi}_\gamma) - \delta(\boldsymbol{\xi}' - \boldsymbol{\xi}_\gamma) - \delta(\boldsymbol{\xi}_*' - \boldsymbol{\xi}_\gamma)$, $\delta(\boldsymbol{\xi})$ – delta-function. For the evaluation of (4), the domain $\Omega\times\Omega\times 2\pi\times 1$ in R^8 space is considered. The values $\boldsymbol{\xi}_{\alpha_v}, \boldsymbol{\xi}_{\beta_v}, \varepsilon_v, b_v$ are chosen so that $\boldsymbol{\xi}_{\alpha_v}$ and $\boldsymbol{\xi}_{\beta_v}$ lie inside the Ω domain and coincide with nodes of the Cartesian grid. Excluding all R^8 grid points with ε_v, b_v resulting in post-collision velocities falling outside Ω, we obtain a 8-dimensional integration grid with N_v nodes. Generally, the post collision velocities $\boldsymbol{\xi}_{\alpha_v}'$ and $\boldsymbol{\xi}_{\beta_v}'$ do not coincide with the Cartesian grid nodes, therefore a regularization is required. We use the conservative regularization method [5] accurate for the Maxwell distribution function.

Suppose that $\boldsymbol{\xi}_{\lambda_v}$ and $\boldsymbol{\xi}_{\mu_v}$ are the nearest nodes of the Cartesian grid for $\boldsymbol{\xi}'_{\alpha_v}$ and $\boldsymbol{\xi}'_{\beta_v}$. Let $\boldsymbol{\xi}_{\lambda_v+s}$ and $\boldsymbol{\xi}_{\mu_v-s}$ be nodes placed symmetrically at the opposite side of the collision sphere with diameter g and center $(\boldsymbol{\xi}_{\alpha_v} + \boldsymbol{\xi}_{\beta_v})/2$. The first step is to replace the post-collision part of $\phi(\boldsymbol{\xi}_\gamma)$ as

$$\delta(\boldsymbol{\xi}'_{\alpha_v} - \boldsymbol{\xi}_\gamma) = (1 - r_v)\delta(\boldsymbol{\xi}_{\lambda_v} - \boldsymbol{\xi}_\gamma) + r_v\delta(\boldsymbol{\xi}_{\lambda_v+s} - \boldsymbol{\xi}_\gamma) ,\ \delta(\boldsymbol{\xi}'_{\beta_v} - \boldsymbol{\xi}_\gamma) = (1 - r_v)\delta(\boldsymbol{\xi}_{\mu_v} - \boldsymbol{\xi}_\gamma) + r_v\delta(\boldsymbol{\xi}_{\mu_v-s} - \boldsymbol{\xi}_\gamma) .$$

This means that contributions at the points ξ'_{α_ν} and ξ'_{β_ν} are distributed between neighboring nodes. Defining the energies $E_0 = (\xi'_{\alpha_\nu})^2 + (\xi'_{\beta_\nu})^2$, $E_1 = (\xi_{\lambda_\nu})^2 + (\xi_{\mu_\nu})^2$, $E_2 = (\xi_{\lambda_\nu+s})^2 + (\xi_{\mu_\nu-s})^2$, we can see that due to the aforementioned choice of neighbors one of the following inequalities is satisfied: $E_1 \le E_0 < E_2$ or $E_2 < E_0 \le E_1$. Introduce the coefficient r_ν in accordance with the energy conservation law using the relation $E_0 = (1 - r_\nu)E_1 + r_\nu E_2$, $0 \le r_\nu < 1$. Consequently, the value of $f'_{\alpha_\nu} f'_{\beta_\nu}$ can be found by the interpolation $f'_{\alpha_\nu} f'_{\beta_\nu} = (f_{\lambda_\nu} f_{\mu_\nu})^{1-r_\nu} \cdot (f_{\lambda_\nu+s} f_{\mu_\nu-s})^{r_\nu}$.

The second step is to calculate the integral (4) in all the nodes of the velocity grid $\{\xi_\gamma\}$ as a 8-dimensional sum. Denoting $B = N_0 dv^3 2\pi/4N_c$ and $\Delta_\nu = (f_{\alpha_\nu} f_{\beta_\nu} - f'_{\alpha_\nu} f'_{\beta_\nu}) g_\nu b_\nu$ (dv is the velocity discretization step, $N_c = N_\nu/N_0$), we obtain the approximation of $J(t, \mathbf{x}, \xi_\gamma)$

$$J_\gamma = B \sum_{\nu=1}^{N_\nu} [-(\delta_{\gamma\alpha_\nu} + \delta_{\gamma\beta_\nu}) + (1 - r_\nu)(\delta_{\gamma\lambda_\nu} + \delta_{\gamma\mu_\nu}) + r_\nu (\delta_{\gamma\lambda_\nu+s} + \delta_{\gamma\mu_\nu-s})]\Delta_\nu , \tag{5}$$

where δ_{ij} is the Cronecker symbol.

Note that the aforementioned 8-dimensional grid consisting of N_ν nodes can be obtained in different ways. Particularly, the Korobov method of cubature grids building or the Monte-Carlo method can be used [5]. The first method is more accurate because it provides regular distribution of nodes. After calculation of nodes in a unit 8-dimensional cube and appropriate scaling, the nearest Cartesian nodes are calculated inside the $\Omega\times\Omega$ domain so that all grid nodes with ε_ν, b_ν resulting in post-collision velocities outside Ω are excluded. Finally we obtain a set of collisional parameters $\{\alpha_\nu, \beta_\nu, \lambda_\nu, \mu_\nu, \lambda_{\nu+s}, \mu_{\nu-s}, r_\nu, g_\nu, b_\nu\}$ that can be used at each time step in all grid nodes in the physical space. At the next time step collisional parameters should be recomputed using new 8-dimensional grid.

The set of N_0 equations (3) can be numerically solved by the splitting method. The flux derivative is approximated by the explicit first- or second-order accurate flux conservative scheme in the framework of the finite volume approach

$$\frac{f_{\gamma i}^{j+1} - f_{\gamma i}^{j}}{\Delta t} + \frac{F_{\gamma i+1/2}^{j} - F_{\gamma i-1/2}^{j}}{\Delta x_i} = 0 , \tag{6}$$

where $f_{\gamma i}^{j}$ is distribution function at the γ-th node in the i-th cell (centered at the node x_i) at the time moment $j\Delta$t, $F_\gamma = \xi_{x\gamma} f_\gamma$ is the flux function, $F_{\gamma i+1/2}^{j}$ is the numerical flux on the cell boundary. For calculation of the numerical flux, the Godunov method can easily be applied to the linear advection equation. The second-order accurate scheme ($O(\Delta x^2)$ out of extrema and discontinuities) is obtained using the TVD reconstruction procedure with the minmod-type limiter function [6]. The time step is limited by the Courant condition: $\Delta t = CFL \min(\Delta x_i)/V_{\max}$, where CFL is the Courant number, Δx_i is the cell size. Note that the second-order scheme provides solutions of essentially higher accuracy on realistic computational grids. Disadvantage of this scheme is occurrence of temperature oscillations in low-density regions close to the gas leading edge due to variations of numerical diffusion in the velocity space. This problem should be solved by adjusting of the numerical diffusion.

Comparing of the first- and second-order accurate time integration methods we found that it is convenient to use the symmetric method consisting of three steps: transitional step during $\Delta t/2$, relaxation step during Δt, and transitional step during $\Delta t/2$. This method allows us to use only two arrays of variables at the time layers t and $t + \Delta t$. Using this time integration method we obtain the algorithm with the discretization error $O(\Delta t, \Delta x)$ or $O(\Delta t, \Delta x^2)$; the Courant condition is $CFL \le 2$ in the first case and $CFL \le 1$ in the second case.

The collisional part can be solved using the scheme

$$f_{\gamma i}^{j+\nu/N_\nu} = f_{\gamma i}^{j+(\nu-1)/N_\nu} + \Delta t \Delta_{\gamma\nu i}^{j+(\nu-1)/N_\nu} , \tag{7}$$

where $f_{\gamma i}^{j+\nu/N_\nu}$ is the intermediate variable, $\Delta_{\gamma\nu i}^{j+(\nu-1)/N_\nu}$ is the ν-th member of the sum (5). Therefore, calculation of the total sum (5) is replaced by gradual changing of the distribution function (7) after each collision. Such a scheme is found to be accurate enough and more robust compared with the collision integral calculation.

For resolution of kinetic processes in general case, the condition $\Delta t < 1$ should be satisfied. If the Ω domain in the velocity space is large enough, the grid in physical space resolves the local mean free path and the Courant condition is satisfied, then the time scale resolution is ensured. Calculations were made under the conditions: $V_{\max} = 6$, the discretization step in the velocity space is $dv = 0.36–0.48$, $N_0 = 8\,000 – 19\,000$. Korobov's and Monte-Carlo integration grids in R^8 space with $N_v = 33\,000 – 65\,000$ nodes were used. The domain in physical space is $0 \le x \le 2\,000$, grids in the physical space contain $360 – 500$ nodes, the initial cell size is $\Delta x_1 = 0.15$, geometrical growth rate factor is 1.01–1.015, so that the condition $\Delta x < \lambda$ is always true. The time step is limited by the condition $CFL = 0.9$. Computational time was varied from 50 to 150 hours using a PC Pentium 4 (3 GHz) system. Refinement of the discretization step in velocity space practically does not affect numerical solutions whereas it diminishes temperature oscillations in the low-density region. The difference between the temperature profiles calculated using grids consisting of 360 and 500 nodes does not exceed 2% in the low-density region.

MODELING RESULTS

The flow structure described with temporal and spatial coordinates includes three main evolution stages: the free-molecular and nearly free-molecular stage, the transitional stage and the continuum stage [2–4]. During the free-molecular and nearly free-molecular stage ($t < 1–3$), the numerical density is a monotonically diminishing function of distance from the surface, since only the fastest particles contribute to the density. The temperature behaves in a similar way. The macroscopic velocity, oppositely, is an increasing function. Due to the lack of collisions, the gas state is non-equilibrium and $T_x \neq T_y$ everywhere. Since the flow is in the x direction, the transversal temperature remains constant: $T_y = 1$ (temperatures T_x, T_y, T are assumed to be dimensionless, T_w is the scale). Comparison of theoretical and numerical results for collisionless flow has been made and showed their good agreement. The similarity parameter for the collisionless flow is $\eta = x/\sqrt{2}t$, in our calculations $\eta \le 3.9$.

Due to the influence of collisions giving growing reverse flux of particles to the surface, the flow loses its self-similarity. As a result, the macroscopic velocity decreases and the density increases near the surface. Distributions of dimensionless parameters: the density, the macroscopic velocity and the flux of particles (the scales are n_e, v_0, $v_0 n_e$) as functions of x and η at $t = 6, 21, 72, 141, 204, 300$ are presented in Fig. 1 (a, b, c, respectively).

Distributions of the density and the macroscopic velocity are not self-similar near $\eta = 0$, while they tend to self-similar distributions at higher η. Regions of self-similarity for these parameters grow with time. Distributions of the flux of particles are almost self-similar in the whole region (especially after the time moment $t = 70$).

The process of translational relaxation can be represented by distributions of temperatures T_y and T_x as functions of the coordinate x. These distributions are shown in Fig. 2 at $t = 21$ (a) and $t = 213$ (b). The position of the gas leading edge is denoted by $x_l = V_{\max} t$. Note that the first-order method gives a significant numerical error in temperature; error can be decreased at the expense of essential computational costs. The temperature T (a) and the Mach number (b) are given in Fig. 3 as functions of x at $t = 6, 21, 72, 141, 204, 300$.

The equilibrium gas state can be identified from the proximity of T_x and T_y profiles. After the time moment $t_c \cong 100$ the quasi-equilibrium region is formed. We can use the criterion $|T_x - T_y|/T \le \varepsilon$ ($\varepsilon = 0.05$) for determination of bounds of the continuum region beginning with the Knudsen layer. In the continuum region, T_x monotonically decreases with x. The Knudsen layer boundary moves to the surface approaching the position $x_{\mathrm{Kn}} \cong 10$. At the time moment $t^* \cong 110$, the Knudsen layer becomes completely subsonic. The external boundary of the continuum region x_c and the position x_m of T_y minimum move away from the surface. The size of the continuum region is also growing with time. After the time moment t^*, the sonic point lies in the continuum region. The boundary of the free-molecular region x_{fm} can be determined from the tendency of the T_y profile to unity. In our calculations, the equality $T_y = 1$ was not reached after the time moment $t \cong 10$ mainly due to boundedness of the velocity space which affects representation of the distribution function «tails». We calculated x_{fm} by extrapolation of the T_y distribution (Fig. 2).

Expressions for $x^*(t)$, $x_c(t)$, $x_m(t)$ and $\eta^*(t)$, $\eta_c(t)$, $\eta_m(t)$, $\eta_{fm}(t)$ are obtained from the numerical data by the least-squares approximations for x (approximations for η are obtained from the definition of η) as

$$x^*(t) = 0.89t^{0.61}, \quad \eta^*(t) = 0.63t^{-0.39}, \quad 20 < t < 300 \qquad x_c(t) = 0.025t^{1.71}, \quad \eta_c(t) = 0.018t^{0.71}, \quad 100 < t < 300$$

$$x_m(t) = 0.81t^{1.18}, \quad \eta_m(t) = 0.57t^{0.18}, \quad 20 < t < 300 \qquad \eta_{fm} = 3.6 \div 3.8, \quad t > 120$$

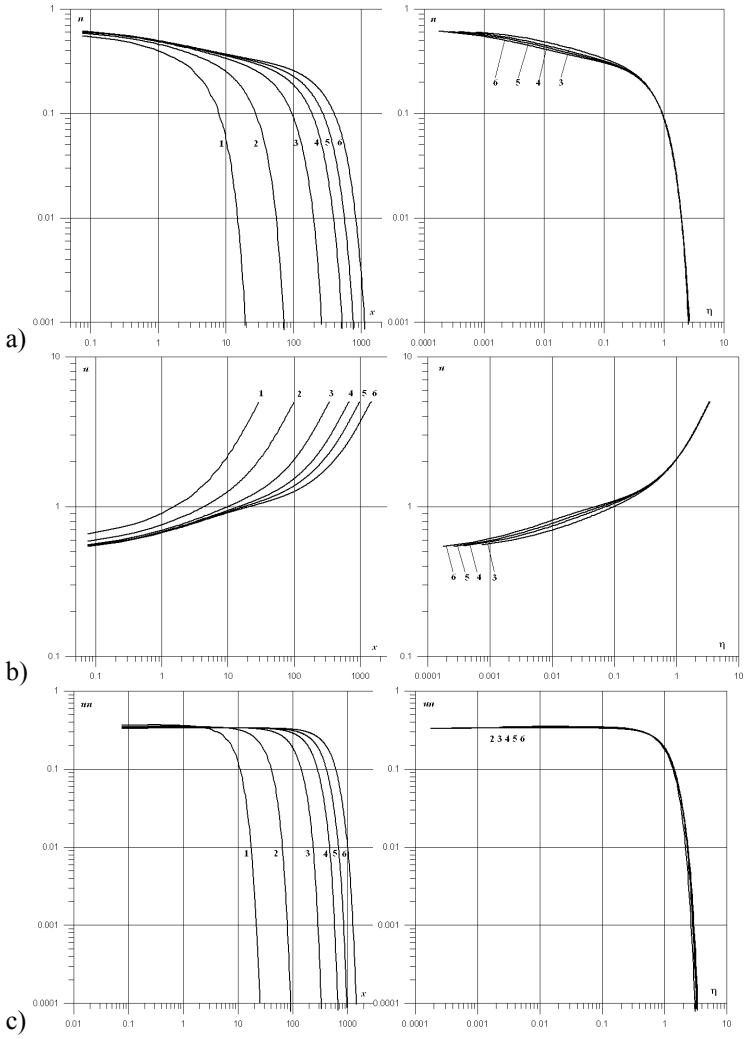

FIGURE 1. Distributions of density n (a), macroscopic velocity u (b), flux of particles un (c) as functions of x and η at t = 6 (1), 21 (2), 72 (3), 141 (4), 204 (5), 300 (6).

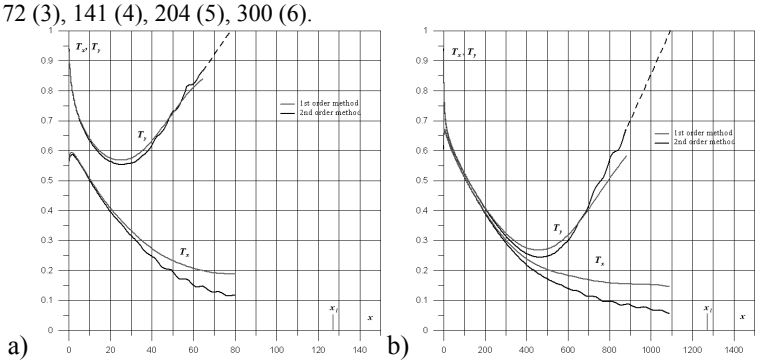

FIGURE 2. Distributions of temperatures T_x and T_y as functions of x at t = 21 (a), 213 (b).

The results described can be generalized in the form of dependencies of characteristic scales in x and η from time. Fig. 4 shows the flow structure in coordinates (t, x) (a) and (t,η) (b). The boundary of vapor sublayer of thickness $\sim\lambda_w$ is marked in Fig. 4 b as η_{fw}. This form clarifies the representation of time and space scales. Aforementioned flow stages are marked in Fig. 4 b. Here F denotes the free-molecular and near free-molecular regime, T – the transitional regime and C – the continuum regime. Such a representation can be useful for the formulation of surface boundary conditions for continuum media equations and for vacuum technology applications.

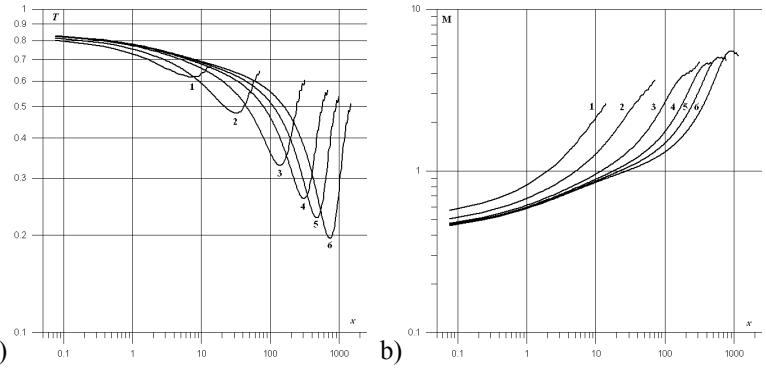

FIGURE 3. Distributions of temperature T (a) and Mach number M (b) as functions of x at t = 6 (1), 21 (2), 72 (3), 141 (4), 204 (5), 300 (6).

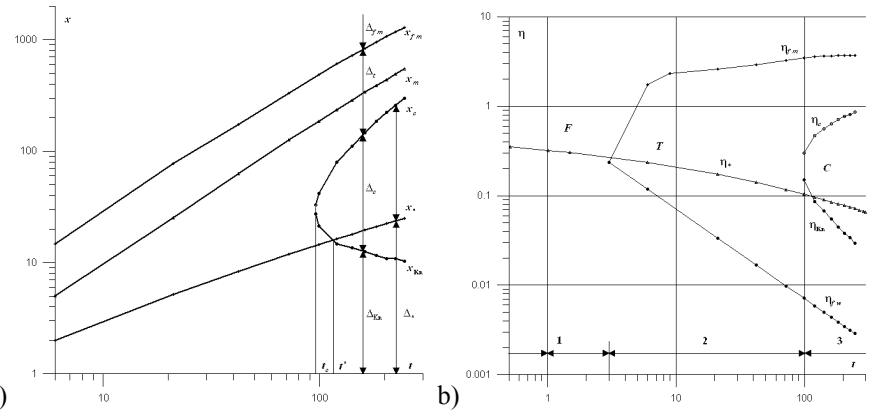

FIGURE 4. The generalized flow structure in coordinates (t, x) (a) and (t, η) (b).

CONCLUSIONS

Our paper deals with the numerical analysis of unsteady vapor outflow from a flat surface on the basis of direct numerical solution of the Boltzmann equation. Dependencies of flow parameters from temporal and spatial coordinates are obtained, flow scales are extracted and analyzed. The generalized gas-dynamic flow structure is presented. The data obtained are in good qualitative agreement with those of Ref. [4]. Issues concerning the robust numerical algorithm construction are discussed.

ACKNOWLEDGMENTS

The authors are thankful to F.G. Tcheremissine for helpful discussions and advice.

The research was supported by The Program of State Support for the Leading Scientific Groups, grant # 4272.2006.1.

REFERENCES

1. G.A. Bird, *Molecular Gas Dynamics and the Direct Simulation of Gas Flows*, Clarendon Press, Oxford, 1994.
2. S.I. Anisimov, *Sov. Phys. JETF*, **27**, 182-184 (1968).
3. D. Sibold and H.M. Urbassek, *Physical Review A*, **43**, 6722-6734 (1991).
4. G.A. Lukyanov, «Unsteady Outflow of the Vapour into Vacuum from the Flat Surface», Proc. of 24th International Symposium on Rarefied Gas Dynamics, pp. 638-643 (2004).
5. F. Tcheremissine, «Direct Numerical Solution of the Boltzmann Equation», Proc. of 24th International Symposium on Rarefied Gas Dynamics, pp. 677-685 (2004).
6. A.G. Kulikovskii, N.V. Pogorelov, A.Yu. Semenov, *Mathematical Aspects of Numerical Solution of Hyperbolic Systems*, Chapman&Hall/CRC, 2001.
7. M.N. Kogan, *Rarefied Gas Dynamics*, Plenum Press, New York, 1969.